High-pressure phases of $FeTiO_3$ from first principles

N. C. Wilson
CSIRO Division of Minerals, Bayview Avenue, Clayton 3168, Australia
and Applied Physics, School of Applied Sciences, RMIT University, G. P. O. Box 2476V, Melbourne, 3001, Australia

S. P. Russo
Applied Physics, School of Applied Sciences, RMIT University, G. P. O. Box 2476V, Melbourne, 3001, Australia

J. Muscat*
CCLRC Daresbury Laboratory, Daresbury, Warrington, WA4 4AD, United Kingdom

N. M. Harrison
Department of Chemistry, Imperial College of Science and Technology, London, SW7 2AY, United Kingdom
and CCLRC Daresbury Laboratory, Daresbury, Warrington, WA4 4AD, United Kingdom
(Received 22 February 2005; revised manuscript received 2 May 2005; published 19 July 2005)

The structural, elastic, and electronic properties of the high-pressure $FeTiO_3$ polymorphs and their relative phase stability under pressure are investigated using hybrid exchange density functional theory. For the currently known phases the computed structural and elastic parameters are in good agreement with those observed, as is the predicted stability of the phases. The transformation of the perovskite polymorph to a new high-pressure polymorph with space group *Cmcm* is predicted to occur at 44 GPa at 0 K.

DOI: 10.1103/PhysRevB.72.024110 PACS number(s): 61.50.Ah, 61.50.Ks

I. INTRODUCTION

$FeTiO_3$ is a transition metal oxide where the partially occupied *d* shells of the cations allow for a range of charge and spin states, resulting in a rich phase diagram of magnetic, electronic, and structural transitions.

Two cation charge orderings are consistent with O^{2-} anions, namely, $Fe^{2+}Ti^{4+}$ and $Fe^{3+}Ti^{3+}$, in which Fe has *d*-electron configurations of d^6 and d^5, respectively. In each of these combinations Fe can exist in a high-spin or low-spin state. As $FeTiO_3$ may exist in this range of possible charge and spin configurations, the theoretical investigation of the high-pressure polymorphic phases requires a careful study of the energetics of the possible Fe and Ti charge and spin combinations and their interaction with the structural degrees of freedom.

Ilmenite, the mineral form of $FeTiO_3$, is commonly found as an inclusion in kimberlites, a type of igneous rock. The ilmenite inclusions are incorporated into the kimberlites at depths of up to 400 km (12–13 GPa), but the exact depth is not well known and therefore an understanding of the high-pressure physics of $FeTiO_3$ could aid in constraining the depth from which they originate.[1] The Fe^{2+} to Fe^{3+} ratio in ilmenite under pressure has been studied experimentally as an indicator of the oxidation state of the host kimberlites, which is used to determine the origin and genesis of diamond deposits.[2]

In addition to ilmenite, two other polymorphs of $FeTiO_3$ are known,[3] namely, the lithium niobate and perovskite structures. The lithium niobate phase forms as a quench product of the perovskite phase which is stable only at pressures greater than 16 GPa. It is presumed that the lithium niobate phase is the favored quench product of the perovskite phase due to kinetic restrictions, as this transition only requires rotation of the oxygen octahedra, whereas transition to the ilmenite structure requires cation rearrangement. The lithium niobate structure is only metastable at atmospheric pressure and will revert to the ilmenite structure at temperatures of 1200 K.[1] Shock-Hugoniot experiments on natural ilmenite have demonstrated that the perovskite structure phase-separates into a mixture of FeO and TiO_2 at pressures greater than 65 GPa.[4]

Several other oxides with ABO_3 stoichiometry transform from the ilmenite structure to a perovskite structure under pressure. Examples of these are the germanates $ZnGeO_3$ and $MgGeO_3$,[5] the titanates $ATiO_3$ (A=Mg, Mn, Cd),[6,7] and the silicate $MgSiO_3$. Recently there has been considerable interest in the discovery of a new high-pressure $CaIrO_3$-type "postperovskite" phase of $MgSiO_3$,[8,9] due to its implications for the geology of the lower mantle of the Earth. This discovery was inspired by the observation of a $CaIrO_3$-type postperovskite phase in Fe_2O_3,[10,11] which transforms from the corundum to perovskite and then to the $CaIrO_3$ phase under increasing pressure. The structural similarity of $FeTiO_3$ to Fe_2O_3 and $MgSiO_3$ and their respective polymorphs suggests that a similar phase could also exist for $FeTiO_3$.

In the present study hybrid exchange density functional theory is used to investigate the structure and electronic properties of the high-pressure polymorphs of $FeTiO_3$. The paper is organized as follows. Section II contains a description of the crystallography of the $FeTiO_3$ polymorphs. Section III describes the computational method used. Structural relaxation data, elastic constants, and charge states for the lithium niobate, perovskite, and $CaIrO_3$-type postperovskite phases are given in Sec. IV and discussed in Sec. VI. The phase stability of all the polymorphs is given in Sec. V and conclusions are summarized in Sec. VI.

 ©2005 The American Physical Society

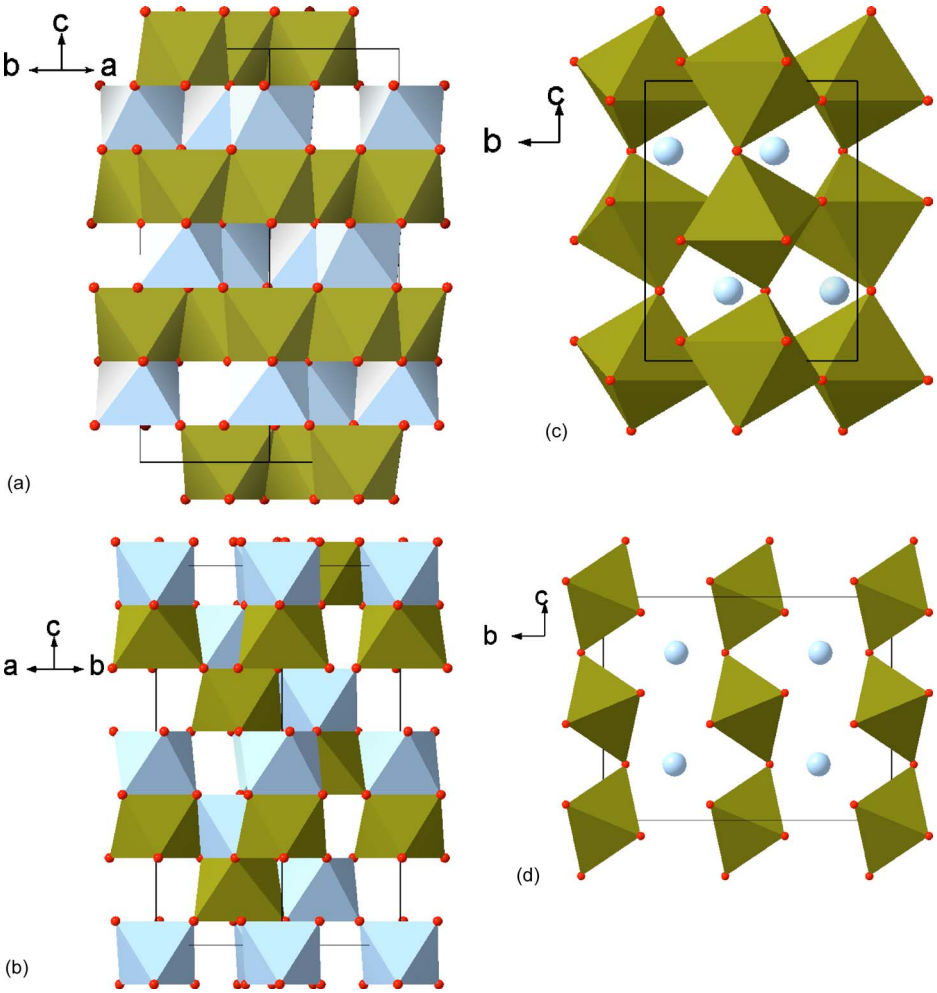

FIG. 1. (Color online) The structures of the $FeTiO_3$ polymorphs studied: (a) ilmenite, (b) $LiNbO_3$, (c) perovskite, and (d) $CaIrO_3$-type postperovskite polymorphs. Dark octahedra represent TiO_6, light octahedra show FeO_6, and Fe ions are shown as large spheres.

II. POLYMORPHS OF $FeTiO_3$

A. Ilmenite

Ilmenite is the naturally occurring form of $FeTiO_3$ and hence the most stable polymorph at ambient temperatures and pressures. The ilmenite structure is based on a hexagonal-close-packed oxygen lattice with metal atoms occupying two-thirds of the available octahedral sites to form honeycomblike layers of edge-shared octahedra. Octahedra in adjacent (001) layers share faces to form dimers, which are separated by empty octahedra along [001], illustrated in Fig. 1. Layers of Fe and Ti alternate with a cation ordering of -Fe-Ti-□-Ti-Fe- along the *c* axis. The hexagonal representation of the unit cell is defined by the **a** and **c** lattice vectors and contains six $FeTiO_3$ units, with Fe ions at (0, 0, 0.3554), Ti ions at (0, 0, 0.1466), and O at (0.3172, 0.0235, 0.2449). X-ray diffraction measurements[12] give values of $\mathbf{a}=5.0875$ and $\mathbf{c}=14.0827$ Å, with a $\mathbf{c}/\mathbf{a}$ ratio of 2.77. Ilmenite responds anisotropically under pressure, being more compressible in the **c** direction because of the vacancies that alternate with the cations, leading to a decrease in the $\mathbf{c}/\mathbf{a}$ ratio with increasing pressure.

B. Lithium niobate

The lithium niobate differs from the ilmenite structure only in that it has layers of mixed Fe and Ti ions and a *c*-axis ordering of -Fe-Ti-□-Fe-Ti-, with a space group of $R3c$ (Fig. 1). As for ilmenite, the structure is defined by the **a** and **c** lattice vectors and contains two $FeTiO_3$ units, but with the Fe ions at $(0,0,u)$ and $(0,0,u+\frac{1}{2})$, Ti ions at (0,0,0) and $(0,0,\frac{1}{2})$, and the O ions at (x,y,z), $(\bar{y},x-y,z)$, $(\bar{x}+y,\bar{x},z)$, $(\bar{y},\bar{x},z+\frac{1}{2})$, $(\bar{x}+y,y,z+\frac{1}{2})$, and $(x,x-y,z+\frac{1}{2})$. X-ray diffraction measurements[1] give unit cell parameters of $\mathbf{a}=5.12$ and $\mathbf{c}=13.76$ and internal coordinates $u=0.287$, $x=0.0449$, $y=0.3446$, and $z=0.0641$. Compared to the ilmenite structure the octahedra in the lithium niobate form are contracted along the **c** direction, with the niobate structure having a smaller **c** lattice parameter.

C. Perovskite

At high pressures, $FeTiO_3$ forms an orthorhombic perovskite phase with the gadolinium ferrite ($GdFeO_3$) type structure,[3] a distortion of the cubic perovskite structure, with space group *Pbnm*, as shown in Fig. 1. In the perovskite structure there are two distinct cation sites and typically the smaller cation is octahedrally coordinated with oxygen at positions $(\frac{1}{2},0,0)$, with the larger cation in the larger 12-coordinated site $(u,v,\frac{1}{4})$. In the $GdFeO_3$ structure, tilting of the octahedra results in a lowering of the coordination of the large cation site from 12 to 8. The unit cell contains four

TABLE I. Energy differences (relative to lowest-energy state per $FeTiO_3$ formula unit in eV) and Mulliken population analysis of ionic net charge $(\alpha+\beta)$ and net spin $(\alpha-\beta)$ for lithium niobate phase at 0 GPa, computed within the B3LYP approximation.

State	Energy difference	Ionic net charge			Net spin		
		Fe	Ti	O	Fe	Ti	O
Fe^{2+}	0.000	1.77	2.31	−1.36	3.80	−0.10	0.10
Fe^{3+}	2.138	2.11	2.10	−1.40	4.27	0.95	0.26

$FeTiO_3$ units with O ions at $\pm(xyz;\frac{1}{2}-x,y+\frac{1}{2},\frac{1}{2}-z;\bar{x},\bar{y},z+\frac{1}{2};x+\frac{1}{2},\frac{1}{2}-y,\bar{z})$. Based on the measured volume changes Leinenweber *et al.*[3] have proposed that no charge transfer occurs during the transition from ilmenite to the perovskite phase, with the iron remaining divalent and the titanium tetravalent. The observed equation of state[1] extrapolated to absolute zero gives the ilmenite to perovskite phase transition at 25±4 GPa, while the lithium niobate phase transforms to the perovskite phase at 17±7 GPa.

D. $CaIrO_3$-type postperovskite phase

The proposed postperovskite phase investigated here is an orthorhombic structure based on the $CaIrO_3$ structure with space group *Cmcm*,[13] shown in Fig. 1. It has two distinct cation sites, one sixfold coordinated and the other eightfold. Ti ions are in the sixfold-coordinated sites, with the octahedra forming an edge-sharing chain as in the rutile structure. The Fe ions occupy eightfold-coordinated sites.

E. Dissociation phases

At high pressures the perovskite phase separates to a mixture of "FeO" and TiO_2.[4] Leinenweber *et al.*[3] predicted this TiO_2 phase to have a baddelyite structure as this was the densest known phase of TiO_2 at the time. More recent studies[14,15] have found the cotunnite structure stable at pressures above 60 GPa, making this a possible dissociation phase.

The baddeleyite unit cell contains four TiO_2 units, and is the stable form of TiO_2 at about 20 GPa.[16] It has space group $P2_1/c$ with Ti and O ions at $\pm(x,y,z;\bar{x},y+\frac{1}{2},\frac{1}{2}-z)$. The lattice vectors at 0 GPa, extrapolated from x-ray diffraction experiments, are $\mathbf{a}=4.662$ Å, $\mathbf{b}=4.969$ Å, $\mathbf{c}=4.911$ Å, and $\beta=99.4°$. The cotunnite structure has space group *Pnma*, with experimentally measured lattice parameters $\mathbf{a}=5.52$ Å, $\mathbf{b}=5.30$ Å, and $\mathbf{c}=5.60$ Å at 61 GPa and the FeO phase has a rocksalt structure (space group *Fm3m*), with Fe ions at (0,0,0) and O ions at $(\frac{1}{2},\frac{1}{2},\frac{1}{2})$.

III. METHOD

All calculations were performed using the CRYSTAL software[17] which is based on the periodic, linear combination of atomic orbitals formalism where the Bloch orbitals of the crystals are expanded using atom-centered Gaussians orbitals with s,p, or d symmetry.

TABLE II. Mulliken population analysis of total charge $(a+b)$ and net spin $(a-b)$ for the cations in the Fe^{2+}-Ti^{4+} state computed within the B3LYP approximation for the high-pressure polymorphs.

Orbital	Fe		Ti	
	Charge	Spin	Charge	Spin
	Lithium niobate			
dz^2	1.84	0.14	0.34	−0.03
dxz	1.08	0.91	0.17	−0.01
dyz	1.08	0.91	0.17	−0.01
dx^2-y^2	1.08	0.91	0.18	−0.01
dxy	1.08	0.91	0.18	−0.01
	Perovskite			
dz^2	1.12	0.87	0.39	0.00
dxz	1.05	0.94	0.25	0.00
dyz	1.09	0.90	0.23	−0.10
dx^2-y^2	1.50	0.49	0.24	−0.10
dxy	1.45	0.53	0.39	0.00
	$CaIrO_3$- type post perovskite			
dz^2	1.10	0.894	0.37	0.0
dxz	1.09	0.894	0.25	0.0
dyz	1.07	0.912	0.32	−0.04
dx^2-y^2	1.80	0.157	0.24	−0.04
dxy	1.12	0.866	0.41	0.01

Becke's three-parameter hybrid functional[18] (B3LYP) was used to approximate electronic exchange and correlation. B3LYP is implemented in the CRYSTAL package using the modified form of Becke's three-parameter hybrid functional as employed by Stephens *et al.*[19] Within this approximation the exchange-correlation energy is $E_{XC}=(1-a_0)E_X^{LDA}+a_0E_X^{HF}+a_X\Delta E_X^{B88}+a_cE_C^{LYP}+(1-a_c)E_C^{VWN}$ where $a_x\Delta E_X^{B88}$ is Becke's gradient correction to the exchange functional,[20] E_X^{HF} is the Fock exchange energy, and the correlation (E_c) is given by a combination of the Lee, Yang, and Parr[21] (LYP) and the Vosko, Wilk, and Nussair[22] (VWN) functionals. Values for a_0,a_x and a_c are 0.2, 0.72, and 0.81, respectively, as given by Becke.[23] Solid state calculations using this functional have been shown to yield band structure[24] and structural properties[25] in excellent agreement with experiment. Of particular relevance to the current study is that, unlike the local density or generalized gradient approximation functionals, a qualitatively correct ground state is obtained for a wide range of transition metal oxides.[26–29]

The basis sets used here were developed and optimized in previous calculations on rutile TiO_2 and bulk surfaces[14,30–33] and studies of hematite Fe_2O_3,[34] and are the same as used for previous work on ilmenite.[35] The general quality of the basis set is triple valence; that is three independent functions are used to expand the valence electrons of each ionic type. In addition *d*-symmetry functions were introduced on the oxygen ions.[36]

The accuracy of the calculation of the bielectronic Coulomb and exchange series is dependent on the truncation of the atomic orbital overlap integrals. The truncation of these overlap integrals is controlled by five cutoff tolerances do-

TABLE III. Structural parameters of the $FeTiO_3$ lithium niobate phase at 0 GPa, $FeTiO_3$ perovskite phase at 18 GPa, and the postperovskite phase at 50 GPa. Distances are in angstroms and volumes in $Å^3$/formula unit. Solutions converged in the Fe^{2+} state.

					Internal coordinates			Volume
Source	*a*	*b*	*c*	Atom	*x*	*y*	*z*	
				$FeTiO_3$ lithium niobate phase				
B3LYP	5.168		13.899	Ti	0	0	0.287	53.57
				Fe	0	0	0.001	
				O	0.045	0.341	0.063	
Expt.	5.12		13.76			Not given		52.13
				$FeTiO_3$ perovskite phase				
B3LYP	4.966	5.278	7.262	Fe	−0.025	0.072	0.25	47.6
				O1	0.127	0.446	0.25	
				O2	−0.321	0.313	0.064	
Expt. (Ref. 3)	5.026	5.174	7.245			Not given		47.1
				$FeTiO_3$ postperovskite phase				
B3LYP	2.79	8.93	6.82	Fe	0	0.238	0.25	42.5
				O1	0	0.915	0.25	
				O2	0	0.638	0.433	

nated as ITOL1, ITOL2, ITOL3, ITOL4, and ITOL5. In the current study these tolerances were set to $10^{-7}, 10^{-7}, 10^{-7}, 10^{-7}$, and 10^{-14}, respectively, which will typically converge total energy differences between related structures to within 0.1 mHa. Further details of this procedure have been described elsewhere.[37] The reciprocal space integration was performed by sampling the Brillouin zone using the Monkhorst-Pack[17,38] scheme with a shrinking factor of 4. This gives 14 symmetry-nonequivalent points in the irreducible Brillouin zone of the lithium niobate polymorph, and 27 symmetry-nonequivalent points for the perovskite structure.

The lattice parameters and internal coordinates of the $FeTiO_3$ polymorphs were optimized using a modified Broyden-Fletcher-Goldfarb-Shanno[39] algorithm to a tolerance of 0.001 Å in the structure and 10^{-7} Ha per formula unit in the total energy. Calculations at finite pressures were performed by applying a hydrostatic pressure and minimizing the enthalpy with respect to the cell parameters and internal coordinates. The bulk modulus and its pressure derivative were computed by fitting the results from a set of optimizations at six pressure values between 0 and 60 GPa to a Murnaghan equation of state.[40]

IV. STRUCTURAL, ELASTIC, AND ELECTRONIC PROPERTIES

The properties of ilmenite have been extensively studied previously within the Hartree-Fock and B3LYP approximations by Wilson *et al.*[35] It was found that the hybrid-exchange density functional (B3LYP) provided a qualitatively correct description of the ground-state electronic structure and that the predicted geometric and elastic parameters were in close agreement with experiment as was the charge-transfer excitation energy. This previous investigation[35] also found the energy difference between the ferromagnetic and antiferromagnetic solutions to be small, less than 0.03 eV per formula unit, and so in this investigation we have used the ferromagnetic solutions for computational efficiency.

A. Lithium niobate

Initial calculations for the lithium niobate structure were performed at the experimental geometry,[3] with solutions converged for both the Fe^{2+}-Ti^{4+} and Fe^{3+}-Ti^{3+} states within the B3LYP approximation. The total energies are reported in Table I, and show the Fe^{2+} state to be the most stable with the Fe^{3+} state 2.14 eV higher in energy.

Mulliken population analysis of the charge and spin densities reveals the Fe ion to have a ionic net charge of $1.8|e|$ and a net spin of $3.8|e|$ consistent with the Fe ion being in a high-spin d^6 state. For the Fe^{3+}-Ti^{3+} state an electron localizes on the Ti ion and the net spin on the ion increases from about $0|e|$ to $0.95|e|$. Further analysis of the Mulliken results, given in Table II, shows the electron is localized in the Ti dz^2 orbital.

TABLE IV. Bulk moduli measured in GPa for the three high-pressure polymorphs.

Method	Lithium niobate	Perovskite	Postperovskite
B3LYP	191	222	207
Expt.	182±7 (Ref. 1)	211±14 (Ref. 3)	

TABLE V. Energy differences (relative to lowest-energy state per $FeTiO_3$ formula unit in eV) and Mulliken population analysis of ionic net charge ($\alpha+\beta$) and net spin ($\alpha-\beta$) for perovskite phase at 18 GPa, computed within the B3LYP approximation. The notation *LS* refers to Fe in the low-spin configuration and *Small* to Fe in the small cation (six coordinated) site.

		Ionic net charge				Net spin			
State	Energy difference	Fe	Ti	O1	O2	Fe	Ti	O1	O2
Fe^{2+}	0.00	1.71	2.34	−1.36	−1.34	3.73	−0.02	0.08	0.10
Fe^{2+}_{LS}	3.38	1.44	2.32	−1.25	−1.26	0.00	0.00	0.00	0.00
$Fe^{2+}_{Small-LS}$	2.03	1.45	2.32	−1.25	−1.26	0.00	0.00	0.00	0.00
Fe^{3+}_{Small}	2.33	2.01	2.16	−1.38	−1.40	4.16	0.92	0.21	0.23

Relaxation of the structure in the Fe^{2+}, high-spin, state resulted in the geometry reported, and compared to that deduced from x-ray diffraction, in Table III. The unit cell parameters and c/a ratio are found to be within 1% of the experimental values.[3] No experimental values for the internal coordinates are available for comparison with the values predicted here. The calculated bulk modulus, given in Table IV, is 191 GPa which is in excellent agreement with that observed (182±7 GPa).

B. Perovskite

The structure of the perovskite phase was computed at 18 GPa in order to facilitate comparison with the high-pressure observations of Leinenweber *et al.*[3] For the perovskite structure there are two different cation sites; a small octahedrally coordinated site and a large 12-coordinated site. Solutions were converged with the Fe ion in both the small and large cation sites, and Mulliken analysis of the resulting charge and spin densities are presented in Table V. The lowest-energy configuration was found to be with Fe in the large cation site, with a high-spin d^6 electron configuration, consistent with the interpretation of the experimental data presented by Leinenweber *et al.*[3]

Not all charge and spin states were stable in this phase. The ionic radii given by Shannon and Prewitt[41] give a larger size for the Ti^{3+} ion than the Fe^{3+} ion, implying that it will be more favorable for Fe in the 3+ state to be located in the small cation site in the perovskite structure. A stable solution was found with the Fe^{3+} in the small cation state but this state has an energy 2.33 eV per formula unit higher than the lowest-energy state found in the current study. A solution with the Fe^{3+} ion in the large cation site would be expected to be even less energetically favorable and was found to be unstable.

The population analysis for the Fe^{2+} state is given in Table II, and confirms a high-spin d^6 configuration. The dz^2, dxz, and dyz are singly occupied while the β-spin electron is accommodated in a combination of the dx^2-y^2 and dxy orbitals.

Structural parameters computed for the perovskite phase with Fe in the large cation site are presented in Table III. In the Fe^{2+} high-spin state the predicted unit cell parameters are in good agreement with those observed. The bulk moduli are given in Table IV and, the computed value of 222 GPa is in good agreement with that observed (211 GPa).

C. $CaIrO_3$-type postperovskite phase

No structural data have been measured for the postperovskite phase in $FeTiO_3$. For this phase, the high-spin Fe^{2+} state was relaxed at 50 GPa resulting in the structural parameters given in Table III. With these structural parameters other charge and spin states were tested. A low-spin Fe^{2+} state was stable, but solutions for the Fe^{3+} configuration were found to be unstable. Table VI gives the relative energies of the high- and low-spin Fe^{2+} states, with the high-spin state being 3.5 eV more favorable. The population analysis given in Table II shows that the dx^2-y^2 orbital is doubly occupied, with the other d orbitals singularly occupied. The computed bulk modulus for this phase is 207 GPa at 0 GPa.

V. PHASE STABILITY

To study the phase stability of the various polymorphs, each of the structures was relaxed in a range of charge and

TABLE VI. Energy differences (relative to lowest-energy state per $FeTiO_3$ formula unit in eV) and Mulliken population analysis of ionic net charge ($\alpha+\beta$) and net spin ($\alpha-\beta$) for the $CaIrO_3$-type "postperovskite" phase at 50 GPa, computed within the B3LYP approximation. The notation *LS* refers to Fe in the low-spin configuration.

		Ionic net charge				Net spin			
State	Energy difference	Fe	Ti	O1	O2	Fe	Ti	O1	O2
Fe^{2+}	0.0	1.73	2.26	−1.31	−1.34	3.74	−0.07	0.09	0.12
Fe^{2+}_{LS}	3.46	1.50	2.26	−1.24	−1.26	0	0	0	0

TABLE VII. Enthalpy and volume changes for the phase transitions ilmenite to lithium niobate (Il $\rightarrow$LN)*a*, ilmenite to perovskite (Il$\rightarrow$Pv), and lithium niobate to perovskite (LN$\rightarrow$Pv). Enthalpy in units of eV per formula unit, volumes in units of A^3 per formula unit.

Source	Il$\rightarrow$LN	Il$\rightarrow$Pv	LN$\rightarrow$Pv
	Change in enthalpy		
B3LYP	0.11	0.33	0.22
Expt. (Ref. 1)	0.14±0.01	0.26±0.04	0.12±0.05
	Change in volume		
	−0.38	−1.75	−1.6
Expt. (Ref. 1)	−0.56	−1.66	1.1

spin states for a set of pressures. This approach will give the relative phase stability of the four polymorphs and disassociation phases considered. At 0 GPa the most stable polymorph of $FeTiO_3$ is found to be ilmenite, with Fe in a low-spin d^6 configuration. The computed pressure dependence of the enthalpies, relative to ilmenite, of the other polymorphs are plotted in Fig. 2.

The ilmenite to perovskite phase transition is predicted to occur at 23 GPa, which is in good agreement with the observed transition pressure, extrapolated to 0 K, of 25±4 GPa.[1] The most stable perovskite phase is predicted to have Fe in the large cation site with a high-spin d^6 configuration. In this perovskite phase structural relaxations were performed for Fe^{2+} in the low-spin configuration in both cation sites, along with Fe^{3+} in the small cation site, none of which were found to be more stable than the high-spin Fe^{2+} configuration in the range of pressures considered here.

The lithium niobate phase, with high-spin Fe^{2+}, is slightly higher in energy than the ilmenite phase (0.1 eV per formula unit at 0 GPa), and is predicted here to transform to the perovskite structure at 17 GPa which is in close agreement with the observed transition pressure, extrapolated to 0 K, of 17±7 GPa.[1] Relaxations were also performed with Fe^{2+} in a low-spin configuration, which was found to become more stable than the high-spin configuration at pressures greater than 43 GPa. This is similar to the high to low spin collapse of Fe seen experimentally in Fe_2O_3,[42] and (Mg, Fe) SiO_3;[43] however, in the case $FeTiO_3$ the lithium niobate phase is not the most stable polymorph at 43 GPa, and it is unlikely that the high- to low-spin transition will be observable.

At 44 GPa, a transition from the perovskite to a $CaIrO_3$-type postperovskite phase is predicted. This transition has not yet been observed for $FeTiO_3$, but is comparable to the observed postperovskite phase of $MgSiO_3$, which was overlooked until recently.[9] The $CaIrO_3$-type postperovskite phase, with high-spin Fe^{2+}, is predicted to be stable, with respect to all phases considered here, until it dissociates into its oxides at 65 GPa.

Ito and Matsui[5] gave a pressure of 20–25 GPa at 1000 °C for the dissociation of $FeTiO_3$ in the perovskite structure to TiO_2 and FeO. In another study, Liu[4] gives a dissociation pressure of 25 GPa at a temperature of 1800 °C on natural samples of ilmenite containing 11% MgO, but also cites unpublished shock experiments that give a dissociation pressure of 65 GPa. Here, the $CaIrO_3$-type postperovskite phase is predicted to decompose to TiO_2 in the cotunnite structure and FeO at 65 GPa, as at this pressure the cotunnite form of TiO_2 is more stable than the baddeleyite. This possibility has

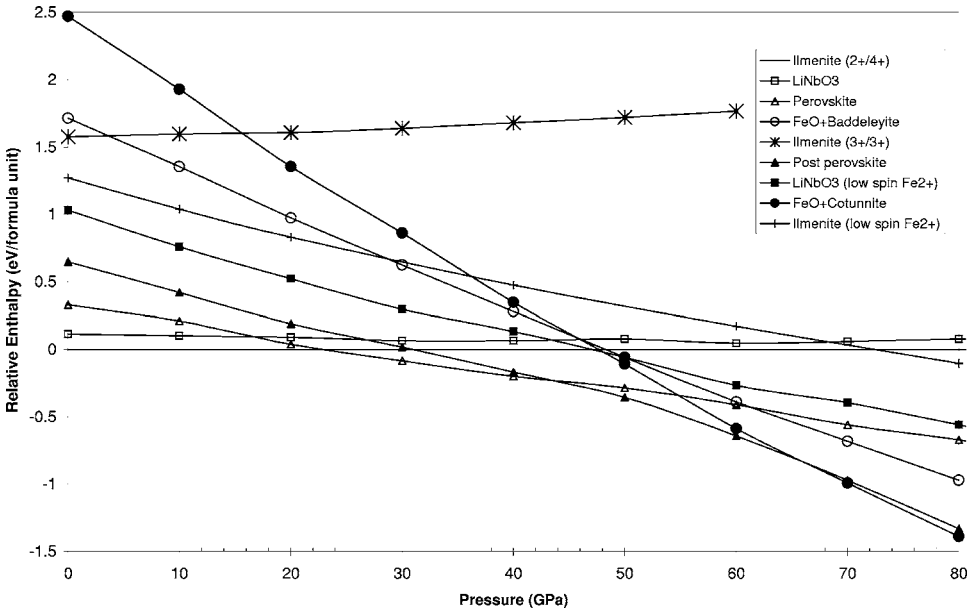

FIG. 2. Phase diagram of $FeTiO_3$ computed within the B3LYP approximation.

not been considered in the interpretation of previous work.

A recent study[2] on natural ilmenite, with minor rutile and hematite impurity phases, found a pressure-induced charge transfer from Fe^{2+}-Ti^{4+} to Fe^{3+}-Ti^{3+}. Earlier experimental studies on synthetic ilmenite[44,45] show that Fe exists in the 2+ state to pressures of at least pressures 18 GPa. The calculations presented here do not show an increase in the stability of the Fe^{3+} for ilmenite with pressure, consistent with the experimental results on synthetic samples. Ilmenite relaxed with a low-spin Fe^{2+} ion does show an increasing stability with pressure, but does not become more stable than ilmenite with a high-spin Fe^{2+} until 73 GPa, well out of the stability range of ilmenite.

Table VII gives enthalpy and volume changes between the various polymorphs. We find that our calculated values are in reasonable agreement with experiment.

VI. CONCLUSION

The prediction of the ground-state electronic configuration of the lithium niobate and perovskite polymorphs of $FeTiO_3$, and hence the prediction of structural parameters, is very sensitive to the treatment of electron exchange and correlation. The hybrid functional B3LYP gives structural and elastic properties in close agreement with experiment. The phase stability and transformation pressures of the ilmenite, lithium niobate, and perovskite structures are in good agreement with experimental results. The existence of a postperovskite phase is predicted, with the transformation from the perovskite phase occurring at 44 GPa, and its dissociation to TiO_2 and FeO occurring at 65 GPa. At the dissociation pressure of 65 GPa, the TiO_2 is predicted to have the cotunnite structure.

The stable phases are all predicted to have high-spin Fe^{2+}. Other spin and charge configurations were optimized at each pressure point, but were found to be higher in energy. No evidence was found for charge transfer in ilmenite with pressure.

ACKNOWLEDGMENT

We would like to acknowledge the Victorian Partnership for Advanced Computing and the Australian Partnership for Advanced Computing for their support of computational resources used in this project.

*Present address: Unilever Research and Development, Port Sunlight Laboratory, Merseyside, CH63 3JW, U.K.

[1] A. Mehta, K. Leinenweber, A. Navrotsky, and M. Akaogi, Phys. Chem. Miner. **21**, 207 (1994).
[2] T. Seda and G. R. Hearne, J. Phys.: Condens. Matter **16**, 2707 (2004).
[3] K. Leinenweber, W. Utsumi, Y. Tsuchida, T. Yagi, and K. Kurita, Phys. Chem. Miner. **18**, 244 (1991).
[4] L. Liu, Phys. Earth Planet. Inter. **10**, 167 (1975).
[5] E. Ito and Y. Matsui, Phys. Chem. Miner. **4**, 265 (1979).
[6] J. A. Linton, Y. Fei, and A. Navrotsky, Am. Mineral. **82**, 639 (1997)
[7] A. Navrotsky, Chem. Mater. **10**, 2787 (1998).
[8] A. R. Oganov and S. Ono, Nature (London) **430**, 445 (2004).
[9] M. Murakami, K. Hirose, K. Kawamura, N. Sata, and Y. Ohishi, Science **304**, 855 (2004).
[10] S. Ono, T. Kikegawa, and Y. Ohishi, J. Phys. Chem. Solids **65**, 1527 (2004).
[11] S. Ono, K. Funakoshi, Y. Ohishi, and E. Takahashi, J. Phys.: Condens. Matter **17**, 269 (2005).
[12] B. A. Wechsler and C. T. Prewitt, Am. Mineral. **69**, 176 (1984).
[13] F. Rodi and D. Babel, Z. Anorg. Allg. Chem. **336**, 17 (1965).
[14] J. Muscat, V. Swamy, and N. M. Harrison, Phys. Rev. B **65**, 224112 (2002).
[15] L. S. Dubrovinsky, N. A. Dubrovinskaia, V. Swamy, J. Muscat, N. M. Harrison, R. Ahuja, B. Holm, and B. Johansson, Nature (London) **410**, 653 (2001).
[16] H. Sato, S. Endo, M. Sugiyama, T. Kikegawa, O. Shimomura, and K. Kusaba, Science **251**, 786 (1991).
[17] V. R. Saunders, R. Dovesi, C. Roetti, R. Orlando, C. M. Zicovich-Wilson, N. M. Harrison, K. Doll, B. Civalleri, I. Bush, Ph. D'Arco, and M. Llunell, *CRYSTAL2003 User's Manual* (University of Torino Press, Torino, 2003).
[18] A. D. Becke, J. Chem. Phys. **98**, 5648 (1993).
[19] P. J. Stephens, F. J. Devlin, C. F. Chabalowski, and M. J. Frisch, J. Phys. Chem. **98**, 11623 (1994).
[20] A. D. Becke, Phys. Rev. A **38**, 3098 (1988).
[21] C. Lee, W. Yang, and R. G. Parr, Phys. Rev. B **37**, 785 (1988).
[22] S. H. Vosko, L. Wilk, and M. Nusair, Can. J. Phys. **58**, 1200 (1980).
[23] A. D. Becke, J. Chem. Phys. **88**, 1053 (1988).
[24] J. Muscat, A. Wander, and N. M. Harrison, Chem. Phys. Lett. **342**, 397 (2001).
[25] N. Wilson and J. Muscat, Mol. Simul. **28**, 903 (2002).
[26] X. B. Feng and N. M. Harrison, Phys. Rev. B **69**, 132502 (2004).
[27] I. D. R. Moreira and R. Dovesi, Int. J. Quantum Chem. **99**, 805 (2004).
[28] D. Munoz, N. M. Harrison, and F. Illas, Phys. Rev. B **69**, 085115 (2004).
[29] X. B. Feng and N. M. Harrison, Phys. Rev. B **69**, 035114 (2004).
[30] J. Muscat, N. M. Harrison, and G. Thornton, Phys. Rev. B **59**, 2320 (1999).
[31] J. Muscat, N. M. Harrison, and G. Thornton, Phys. Rev. B **59**, 15457 (1999).
[32] W. C. Mackrodt, E. A. Simson, and N. M. Harrison, Surf. Sci. **384**, 192 (1997).
[33] N. M. Harrison, X. G. Wang, J. Muscat, and M. Scheffler, Faraday Discuss. **114**, 305 (1999).
[34] M. Catti, G. Valerio, and R. Dovesi, Phys. Rev. B **51**, 7441 (1995).
[35] N. C. Wilson, J. Muscat, D. Mkhonto, P. E. Ngoepe, and N. M. Harrison, Phys. Rev. B **71**, 075202 (2005)
[36] CRYSTAL basis set library, available at http://www.ch.unito.it/ifm/teorica/crystal.html

[37] C. Pisani, R. Dovesi, and C. Roetti, *Hartree-Fock Treatment of Crystalline Systems*, Lecture Notes in Chemistry Vol. 48 (Springer-Verlag, Heidelberg, 1988).
[38] J. D. Pack and H. J. Monkhorst, Phys. Rev. B **16**, 1748 (1977).
[39] P. Spellucci, http://plato.la.asu.edu/donlp2.html
[40] F. D. Murnaghan, Proc. Natl. Acad. Sci. U.S.A. **30**, 244 (1944).
[41] R. D. Shannon and C. T. Prewitt, Acta Crystallogr., Sect. B: Struct. Crystallogr. Cryst. Chem. **25**, 925 (1969).
[42] J. Badro, G. Fiquet, V. V. Struzhkin, M. Somayazulu, H. K. Mao, G. Shen, and T. Le Bihan, Phys. Rev. Lett. **89**, 205504 (2002).
[43] J. Badro, J. P. Rueff, G. Vanko, G. Monaco, G. Fiquet, and F. Guyot, Science **305**, 383 (2004).
[44] C. Boekema, F. Van Der Woude, and G. A. Sawatzky, J. Phys. Colloq. **37**, c-603 (1976).
[45] R. W. Vaughan and H. G. Drickamer, J. Chem. Phys. **47**, 1530 (1967).